

The low frequency density of states and vibrational population dynamics of polyatomic molecules in liquids

Preston Moore

Department of Chemistry, University of Pennsylvania, Philadelphia, Pennsylvania 19104

A. Tokmakoff^{a)}

Department of Chemistry, Stanford University, Stanford, California 94305

T. Keyes

Department of Chemistry, Boston University, Boston, Massachusetts 02215

M. D. Fayer

Department of Chemistry, Stanford University, Stanford, California 94305

(Received 10 March 1995; accepted 24 May 1995)

Instantaneous normal mode calculations of the low frequency solvent modes of carbon tetrachloride (CCl_4) and chloroform (CHCl_3), and experiments on the vibrational population dynamics of the T_{1u} CO stretching mode ($\sim 1980 \text{ cm}^{-1}$) of tungsten hexacarbonyl in CCl_4 and CHCl_3 are used to understand factors affecting the temperature dependence of the vibrational lifetime. Picosecond infrared pump-probe experiments measuring the vibrational lifetime of the T_{1u} mode from the melting points to the boiling points of the two solvents show a dramatic solvent dependence. In CCl_4 , the vibrational lifetime decreases as the temperature is increased; however, in CHCl_3 , the vibrational lifetime actually becomes longer as the temperature is increased. The change in thermal occupation numbers of the modes in the solute/solvent systems cannot account for this difference. Changes in the density of states of the instantaneous normal modes and changes in the magnitude of the anharmonic coupling matrix elements are considered. The calculated differences in the temperature dependences of the densities of states appear too small to account for the observed difference in trends of the temperature dependent lifetimes. This suggests that the temperature dependence of the liquid density causes significant changes in the magnitude of the anharmonic coupling matrix elements responsible for vibrational relaxation. © 1995 American Institute of Physics.

I. INTRODUCTION

The population dynamics of the vibrations of a polyatomic solute molecule in a polyatomic liquid solvent can involve the internal vibrational modes of the solute, the vibrational modes of the solvent, and the low frequency continuum of solvent modes.^{1,2} An initially excited high frequency vibrational mode of a solute molecule can relax by transferring vibrational energy to a combination of lower frequency internal vibrations and solvent vibrations. However, in general, a combination of lower frequency vibrations will not match the initial vibrational frequency. Therefore, one or more quanta of the continuum will also be excited (or annihilated) to make up for the mismatch in the vibrational frequencies and conserve energy.

The low frequency solvent continuum can be described in terms of instantaneous normal modes (INMs).³⁻⁷ For vibrational relaxation in liquids, the INMs play the same role as do phonons in crystals. In a crystal, the phonons provide a continuum of modes that can be created or annihilated to conserve energy in relaxation processes between high frequency vibrations. Because of this similarity, for simplicity we will refer to the INMs as phonons of the liquid or just phonons. It is important to recognize the important differ-

ence between INMs and true crystalline phonons. In a crystal, all phonon modes are bound, giving real phonon frequencies. In a liquid, the structure is continually evolving. Not all of the modes are bound, so that INMs have both real and imaginary frequencies. The imaginary frequency modes are related to the structural evolution of the liquid.⁸

Vibrational relaxation involves a cubic or higher order anharmonic process. The "order" of the process refers to the number of quanta involved in the relaxation. In the simplest cubic anharmonic process, the initial excited vibration is annihilated, a lower frequency internal mode or solvent mode is excited, and a phonon is excited to conserve energy. For a high frequency mode to relax by a cubic process, there must be another high frequency mode close enough in energy for the energy mismatch to fall within the phonon bandwidth. In a quartic or higher order process, the initial vibration is annihilated, two or more lower frequency vibrations are created, and one or more phonons are created to conserve energy. Unless there is a coincidence or Fermi resonance in which energy can be conserved by the creation and annihilation of discrete vibrational modes alone, at least one mode of the low frequency continuum of states will be involved in vibrational population dynamics. The rate constants for vibrational population relaxation dynamics can be described in terms of Fermi's golden rule. Therefore, it is clear that the density of states of the low frequency continuum of INMs will be important in vibrational dynamics.

^{a)}Current address: Technische Universität München, Physik Department E11, James-Frank-Str., 85748 Garching, Germany.

In this paper, we consider the relationship between the density of states of the INMs of two liquids on the vibrational relaxation of a high frequency mode as a function of temperature. The vibrational relaxation dynamics of the T_{1u} CO stretching mode of tungsten hexacarbonyl, $W(CO)_6$, is studied in dilute solution in the liquids carbon tetrachloride, CCl_4 , and chloroform, $CHCl_3$. Picosecond infrared (ir) pump-probe experiments were used to measure the temperature dependence of the vibrational lifetime of the T_{1u} mode.¹ The temperature is varied from the melting points to the boiling points of the two solvents.

The ir pump-probe experiments show that the lifetime of the T_{1u} mode in CCl_4 becomes shorter as the temperature is increased from the melting point to the boiling point. One might be tempted to fit an activation energy to such a temperature dependence. However, when the lifetime is measured in $CHCl_3$ from the melting point to the boiling point, it is observed that the lifetime actually becomes longer as the temperature is increased. This inverted temperature dependence is counterintuitive, yet it has also been observed in other solvents.^{9,10} This temperature dependence clearly demonstrates that a simple description in terms of an activation energy will not account for the change in behavior with solvent. As discussed below, a fully quantum mechanical treatment of vibrational relaxation of polyatomic molecules in polyatomic liquids² cannot account for the inverted temperature dependence. If the relaxation pathway involves a number of high frequency vibrations, whether internal or from the solvent, and a phonon, then the temperature dependence will be determined by the thermal occupation numbers of the modes involved. Since these occupation numbers increase with temperature, the lifetime should get shorter with increasing temperature. The quantum mechanical treatment² and other quantum mechanical¹¹⁻¹⁴ and classical treatments¹⁵⁻¹⁷ of vibrational relaxation do not account for two aspects of the problem that are brought to the fore by the inverted temperature dependence: the temperature dependence of the phonon density of states and the temperature dependence of the magnitude of the anharmonic coupling matrix elements (liquid density dependence).

To gain insights into the temperature dependences of the vibrational lifetimes in the two solvents, the temperature-dependent low frequency INM spectra, $\langle\rho(\omega)\rangle$, of CCl_4 and $CHCl_3$ were calculated. The calculations employed a detailed potential that included intermolecular and intramolecular components. While the low frequency intermolecular modes are of interest here, the potential is able to do a reasonable job of reproducing the vibrational spectrum of the liquids as well. The use of the full potential proved important. Calculations with an accurate Lennard-Jones (LJ) potential do not generate the high frequency “rotational” part of the INM spectrum even though the LJ potential yields the correct melting point of the crystal. The real and imaginary components of the INM spectrum were calculated at three temperatures, near the melting point, at room temperature, and near the boiling point for both solvents. As the temperature is increased, there is a small decrease in the density of states across most of the real part of the spectra with a corresponding increase in the imaginary part.

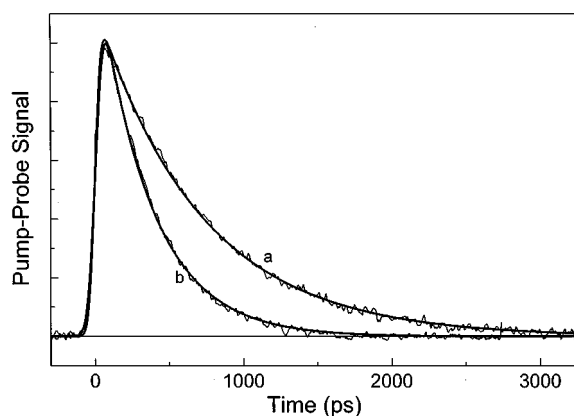


FIG. 1. Pump-probe data of the vibrational relaxation of the T_{1u} CO stretching mode of $W(CO)_6$ in (a) CCl_4 and (b) $CHCl_3$ at $T=295$ K. Single exponential fits convolved with the 40 ps pulses are shown. The vibrational lifetimes for these samples are 700 and 370 ps, respectively.

The paper is laid out in the following manner. In Sec. II, the experimental methods are briefly described, and the experimental results are presented. In Sec. III, the method for calculating the INMs is described, and the results are presented. In Sec. IV, we discuss the results of the experiments and the calculations.

II. EXPERIMENTAL PROCEDURES AND RESULTS

Picosecond pump-probe experiments were performed with mid-ir pulses generated with a $LiIO_3$ optical parametric amplifier (OPA). The laser system is a modified version of a system that has been described in detail previously.¹⁸ The description of the ir pulse generation and pump-probe data collection on the systems discussed here has been described in detail elsewhere.¹

Figure 1 displays pump-probe data taken at 295 K.¹ The data are for (a) $W(CO)_6/CCl_4$ and (b) $W(CO)_6/CHCl_3$. The calculated lines through the data are single exponential fits that include convolution with the pulse shape. The decays can be followed for greater than 4 factors of e . As can be seen from the figure, the data are of very high quality, and the fits are excellent. The vibrational lifetimes for these room temperature samples are 700 and 370 ps, respectively.

When pump-probe experiments are conducted with shorter pulses than those used in these experiments, an additional fast component is observed.¹ For example, room temperature data from $W(CO)_6/CHCl_3$ taken using ~ 2 ps pulses yield a decay time for the fast component of 3.3 ps. The fast decay component is caused by orientational relaxation, which was confirmed using magic angle probing.¹ Although the longer pulses used to obtain the data presented here masks the orientational relaxation, the determination of the vibrational lifetime is not affected. That the pump-probe experiment actually measures the rate of population flow out of the T_{1u} mode has been established for $W(CO)_6/CCl_4$ at room temperature by pumping the $\nu=0\rightarrow 1$ transition and probing at the $\nu=1\rightarrow 2$ frequency.¹⁹ This method, which directly measures the relaxation rate out of $\nu=1$ without a contribution to the signal from ground state recovery, gave a decay

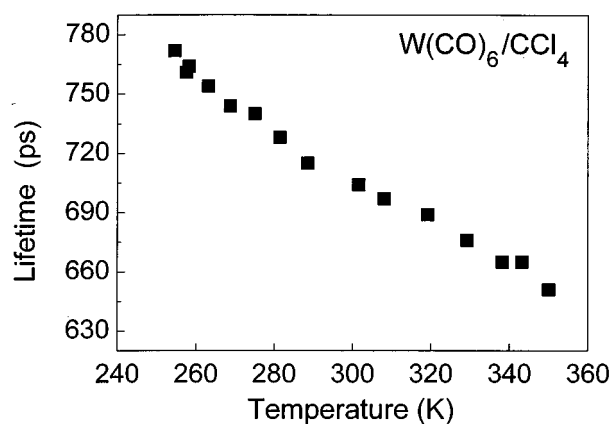


FIG. 2. Temperature dependence of the vibrational relaxation times for the T_{1u} CO stretching mode of $W(CO)_6$ in CCl_4 . The data were taken from the melting point to the boiling point.

time identical to the slow component measured in these experiments at room temperature with the single wavelength pump-probe experiment.

The vibrational relaxation times (T_1) as a function of temperature for T_{1u} mode of $W(CO)_6$ in CCl_4 are shown in Fig. 2. Although the change in the decay with temperature is not large, given the excellent signal-to-noise ratio of the data, the differences are readily discernible. From the melting point to the boiling point, the lifetimes decrease monotonically by 19%. The values range from 775 ps at the melting point (250 K) to 650 ps at the boiling point (350 K). Measurements of T_1 on the T_{1u} mode of $Cr(CO)_6$ in CCl_4 were also made,¹ for which the values range from 400 ps at the melting point to 345 ps at the boiling point.

The results of the pump-probe lifetime measurements of the T_{1u} CO stretching mode of $W(CO)_6$ in $CHCl_3$ are shown in Fig. 3. The decay times are substantially different from those in CCl_4 although the solvents differ only by substitution of a hydrogen for a chlorine. Even more significant is that the basic nature of the temperature dependence is differ-

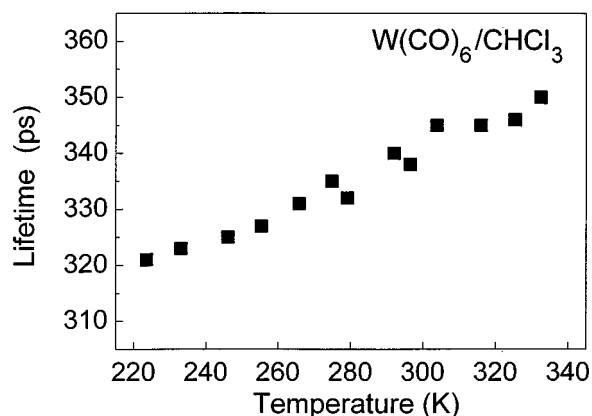


FIG. 3. Temperature dependence of the vibrational relaxation times for the T_{1u} CO stretching mode of $W(CO)_6$ in $CHCl_3$. The data were taken from the melting point to the boiling point. The lifetime actually becomes longer as the temperature is increased (inverted temperature dependence).

ent. Vibrational lifetimes for the T_{1u} mode of $W(CO)_6/CHCl_3$ actually become *longer* as the temperature is increased, changing by 9% from 322 ps at the melting point (210 K) to 350 ps at the boiling point (334 K). This is referred to as the inverted temperature dependence. The difference in the temperature dependences in CCl_4 and $CHCl_3$ will be discussed below in connection with the temperature dependent INM density of states in the two solvents. Measurements of T_1 on the T_{1u} mode of $Cr(CO)_6$ in $CHCl_3$ were also made,¹ for which the values range from 271 ps at the melting point to 253 ps at the boiling point.

III. THE INSTANTANEOUS NORMAL MODE SPECTRA OF CCl_4 AND $CHCl_3$

A. Method of calculation

The density of states for a particular configuration of the liquid, $\rho(\omega;R)$, is obtained by “binning” the square roots of the eigenvalues of the matrix of second derivatives of the potential energy with respect to the mass-weighted coordinates. Negative eigenvalues give imaginary frequencies and their contributions, by convention, are plotted along the $-\omega$ axis. The averaged density of states, $\langle\rho(\omega)\rangle$, is obtained by averaging over R as usual; in our case the configuration average is realized in a molecular dynamics simulation.

The computer simulation of chloroform and carbon tetrachloride involve techniques for constant pressure and constant temperature ensembles.²⁰ These ensembles were simulated using extended systems variables and Nosé–Hoover chains.²¹ Equations of motion for the particles, for the isotropic volume expansion of the box, and for the thermostat were integrated reversibly with breakups of the Liouville Propagator similar to that of Berne *et al.*²¹ The fictitious masses Q and W , for the volume and the thermostat, were set equal to $N_f k_b T w^2$; where N_f is the number of degrees of freedom involved in the coupling, k_b is Boltzmann’s constant, T is the temperature, and w is some characteristic frequency of the motion. We assumed a frequency (w) of 1 ps which allows for fluctuations of the volume and temperature to be controlled on that time scale. Nosé–Hoover chains of length three were also used to ensure ergodic behavior.²² The conserved quantity H' was used to check for accuracy of our particular breakup and during a run was conserved to within 0.01%.

The simulation of 64 carbon tetrachloride and 108 chloroform molecules were carried out using an all atom model with no constraints. This gives a very good representation of the molecules and allows for atomic detail in the potential as well as inter-intramolecular coupling, which are not present in models that employ constraints or united atom methods. The extended system method was used so that the pressure and temperature could be adjusted to the desired values. In the thermodynamic limit of infinite particles a NVE ensemble simulation is identical to a NPT ensemble simulation, but with relatively few particles in our simulation, extended system methods mimic experimental conditions more closely. The simulation potential that we used was that of Dietz and Heinzinger,²³ which gives good agreement with experiments of x-ray and neutron scattering for an all atom

TABLE I. Comparison of model with experiment for vibrations of CHCl_3 .

$\nu(\text{exp}) \text{ cm}^{-1}$	3019	1215	1215	760	760	667	364	260	260
$\nu(\text{fit}) \text{ cm}^{-1}$	3017	1191	1191	767	767	747	313	267	267

model with constraints. The inclusion of intramolecular degrees of freedom does not affect these results.

The intermolecular potential is an atom-atom Lennard-Jones with parameters,

	C-C	Cl-Cl	H-H
sigma (\AA)	3.4	3.44	2.2
epsilon (K)	51.2	150.7	9.995

and the cross terms are calculated with the usual combination rules. A potential including partial charges was tested, with Ewald sums, but did not change our results. The intramolecular interactions are simple harmonic bond stretching and bending potentials of the form

$$V_{\text{bond}}(r) = 1/2 k_{\text{bond}}(r - r_0)^2,$$

$$V_{\text{bend}}(\theta) = 1/2 k_{\text{bend}}(\theta - \theta_0)^2.$$

The equilibrium bond distances and angles are taken from experiment: for CHCl_3 , $r_0(\text{C-Cl}) = 1.758 \text{ \AA}$, $r_0(\text{C-H}) = 1.08 \text{ \AA}$, $\theta_0(\text{Cl-C-Cl}) = 111.3^\circ$, and $\theta_0(\text{H-C-Cl}) = 108.0^\circ$. For CCl_4 , $r_0(\text{C-Cl}) = 1.758 \text{ \AA}$ and $\theta_0(\text{Cl-C-Cl}) = 109.45^\circ$.

With these equilibrium parameters fixed, there are four unknown potential parameters for CHCl_3 and two for CCl_4 . These were determined by a least squares fit to the experimental molecular vibrational frequencies given by Herzberg.²⁴ The results for CHCl_3 are $k_{\text{bond}}(\text{C-Cl}) = k_{\text{bond}}(\text{C-H}) = 360\,000 \text{ K/\AA}^2$, $k_{\text{bend}}(\text{Cl-C-Cl}) = 91\,000 \text{ K/rad}^2$, and $k_{\text{bend}}(\text{H-C-Cl}) = 21\,000 \text{ K/rad}^2$. Comparison with experiment is made in Table I. For CCl_4 , the fit yields $k_{\text{bond}}(\text{C-Cl}) = 148\,000 \text{ K/\AA}^2$ and $k_{\text{bend}}(\text{Cl-C-Cl}) = 73\,900 \text{ K/rad}^2$; comparison with experiment is made in Table II.

The potential assumes purely harmonic motions and ignores the coupling between bends and bonds stretching which accounts for the discrepancy between the experimental frequency and the potential model frequencies. Considering the simplicity of the model, it must be considered to do quite a reasonable job of representing the molecular vibrations.

The simulations were begun with an equilibration run of 50 ps followed by 200 ps of data collection. The equilibration run used "massive" thermostats, which involves a Nosé-Hoover thermostat chain on each degree of freedom. This run achieves, for a given T and P , an equilibrium distribution of orientations, bond lengths, bond angles, and intermolecular distances. Massive thermostats are a quick way to obtain equilibrium distributions since intra-inter molecular coupling is slow. This equilibration phase also allows the

TABLE II. Comparison of model with experiment for vibrations of CCl_4 .

$\nu(\text{exp}) \text{ cm}^{-1}$	790	790	790	635	460	460	460	218	218
$\nu(\text{fit}) \text{ cm}^{-1}$	840	840	840	312	236	236	236	217	217

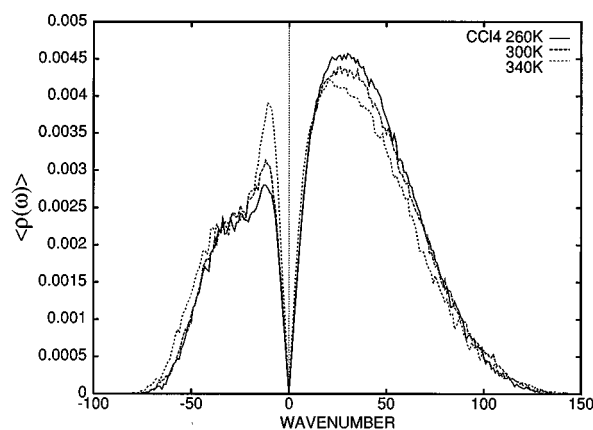


FIG. 4. The low frequency spectra of the instantaneous normal modes of CCl_4 at temperatures of 260, 300, and 340 K, calculated with the full potential. The positive part of the spectrum corresponds to real frequencies, i. e., true oscillatory modes. The negative part of the spectrum corresponds to imaginary frequencies which are related to the structural evolution of the liquid.

volume to equilibrate to the corresponding external pressure. A separate barostat chain allows the volume to fluctuate and ensures ergodic behavior while damping out any sound waves that may be present from the initial conditions or created from the fluctuation of the volume. The pressure of the simulation fluctuated around zero for all the different temperatures. The data collection simulations of 200 ps were carried out with only a global thermostat chain and a separate chain for the volume coordinate. Instantaneous configurations were stored every 2 ps, and $\rho(\omega; R)$ was evaluated.

B. Results

Figure 4 displays the instantaneous normal mode spectrum for CCl_4 at three temperatures calculated with the full potential. The spectrum is shown with both positive and negative values of the frequency. The positive values correspond to the real frequencies and represent true oscillatory modes. The negative part of the spectrum corresponds to imaginary frequencies which are related to the structural evolution of the liquid. The results are presented for three temperatures: 260, 300, and 340 K. These are near the melting point, room temperature, and near the boiling point of CCl_4 , respectively. The maximum phonon frequency is $\sim 130 \text{ cm}^{-1}$, and is essentially temperature independent. The temperature dependence is relatively mild. As the temperature is increased, the density of states of the real part of the spectrum decreases somewhat for most frequencies. Below $\sim 12 \text{ cm}^{-1}$, there is either no change or a small increase with increasing temperature; there is also an increase at the highest frequencies ($\geq 100 \text{ cm}^{-1}$ in CCl_4), where $\langle \rho(\omega) \rangle$ is very small. The imaginary part of the spectrum shows the opposite behavior. As the temperature is increased, the density of states increases, particularly at low frequency, with a pronounced peak appearing at $\sim 10 \text{ cm}^{-1}$. We believe this represents imaginary translational modes, growing in over a background of weakly T -dependent rotational modes. At the peak of the real part of the spectrum ($\sim 30 \text{ cm}^{-1}$), the density

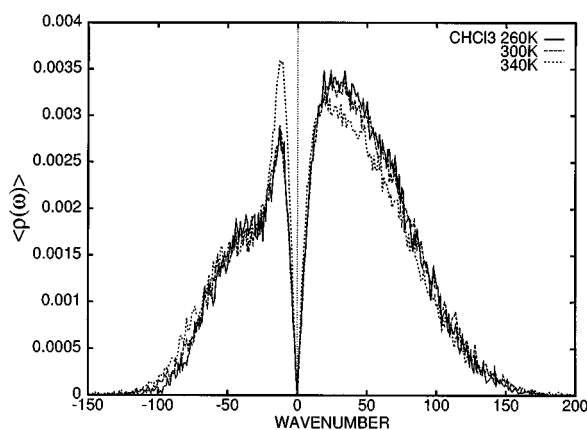


FIG. 5. The low frequency spectra of the instantaneous normal modes of CHCl_3 at temperatures of 260, 300, and 340 K, calculated with the full potential. The positive part of the spectrum corresponds to real frequencies, i.e., true oscillatory modes. The negative part of the spectrum corresponds to imaginary frequencies which are related to the structural evolution of the liquid.

of states decreases $\sim 10\%$ going from 260 to 340 K. A somewhat larger decrease of $\sim 18\%$ is seen at 60 cm^{-1} . At the peak in the imaginary part of the spectrum ($\sim 10 \text{ cm}^{-1}$), the density of states increases $\sim 35\%$ with the increase in temperature. At other frequencies, the change is smaller, e.g., $\sim 19\%$ at 50 cm^{-1} .

Figure 5 displays the calculated instantaneous normal mode spectrum for CHCl_3 at three temperatures. The results are qualitatively very similar to those for CCl_4 . However, the maximum phonon frequency is higher, $\sim 180 \text{ cm}^{-1}$ compared to $\sim 130 \text{ cm}^{-1}$ in CCl_4 . At the peak of the real part of the spectrum ($\sim 30 \text{ cm}^{-1}$), the density of states decreases $\sim 10\%$ going from 260 to 340 K. At 60 cm^{-1} , the decrease is $\sim 13\%$. The increase at the peak of the imaginary part of the spectrum is $\sim 40\%$, and at 50 cm^{-1} , it is $\sim 12\%$. Given the significantly larger noise in the CHCl_3 spectrum, the changes in the density of states with temperature are essentially the same in the two liquids, but there is a significant difference in the maximum phonon frequency.

For comparison with Fig. 4, which was calculated with the full potential, Fig. 6 shows the density of states of CCl_4 calculated using a LJ potential. It can be seen that the LJ potential, while giving qualitatively similar results, does not yield the same spectrum produced by the potential that includes internal degrees of freedom of the molecule. The maximum frequency of both the real and the imaginary parts of the spectrum are substantially lower than seen in Fig. 4. However, the change in the density of states with temperature at the peak of the real part of the spectrum is still $\sim 10\%$. The LJ spectrum probably gives a good description of the true translational spectrum; thus the high- $|\omega|$ modes in both liquids are primarily rotational. This is why CHCl_3 has a higher maximum phonon frequency, with the lighter molecule having higher rotational frequencies.

IV. DISCUSSION

For vibrational relaxation to occur, energy must be conserved. The initially excited vibration must couple its energy

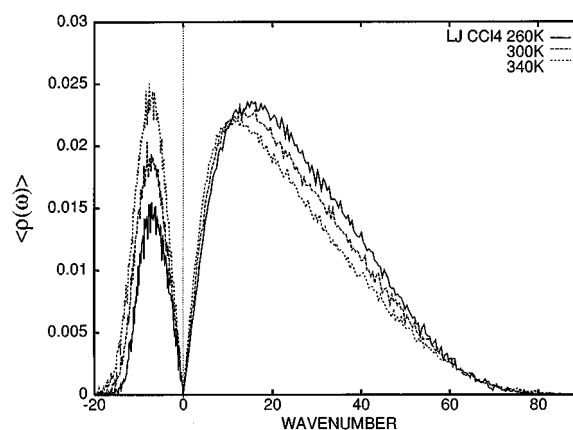


FIG. 6. The low frequency spectra of the instantaneous normal modes of CCl_4 calculated with the Lennard-Jones potential. The substantial difference between this figure and Fig. 4 demonstrates the necessity of using the full potential.

to a combination of lower frequency modes of the solute-solvent system. The combination can involve lower frequency modes of the solute, lower frequency internal vibrational modes of the solvent, and solvent phonons. Vibrational energy can also be transferred to modes of higher frequency, yet this process is generally less efficient than comparable downward pathways.² Barring exceptional circumstances in which there is a coincidence between the initial vibrational energy and a sum of energies of several lower frequency vibrations, a phonon from the continuum of low energy phonon modes will be required to conserve energy. Figure 7 shows a schematic of the fundamental vibrational frequencies of the solute and solvent molecules used in this study. $\text{W}(\text{CO})_6$ has a variety of internal modes that are lower in frequency than the initially excited T_{1u} CO stretching frequency (marked with an asterisk).²⁵⁻²⁹ Both CCl_4 and CHCl_3 have a number of lower energy vibrational modes than the

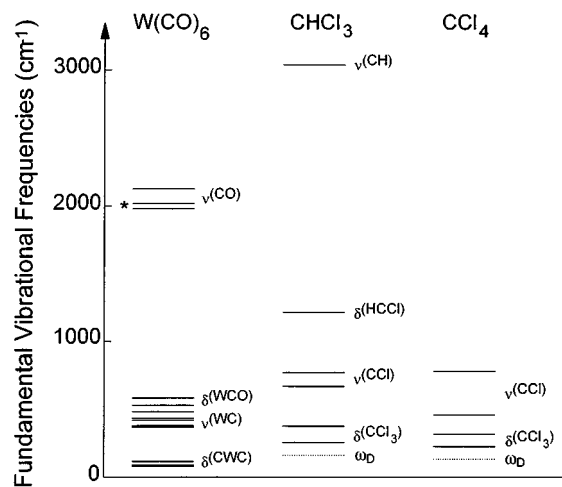


FIG. 7. The fundamental vibrational frequencies and assignments of the solute (Ref. 26) and solvent molecules (Ref. 31). δ and ν refer to bending modes and stretching modes, respectively. The initially excited T_{1u} CO stretching mode is marked with an asterisk. The calculated phonon cutoff frequencies (ω_D) for each liquid is shown with a dotted line.

initially excited mode at $\sim 1980 \text{ cm}^{-1}$.^{30,31} CHCl_3 also has a CH stretching mode at higher energy, $\sim 3020 \text{ cm}^{-1}$, which is too high in energy to participate in the vibrational dynamics. In Fig. 7, the dotted lines labeled as ω_D indicate the approximate cutoff of the INMs of the two solvents.

In the vibrational relaxation of diatomic molecules in pure liquids or in atomic solvents, vibrational relaxation can only occur by coupling to low frequency rotational and translational motions.¹⁵ These high order processes often lead to extremely long vibrational lifetimes, such as in the case of liquid nitrogen where $T_1 = 56\text{s}$.³² For polyatomic molecules in polyatomic solvents, relaxation can occur through much lower order anharmonic processes involving high frequency vibrations of the solute and solvent. We assume that in the relaxation process, the lowest order process possible will dominate. The strength of coupling between participating modes decreases for higher order processes. Thus given that both components of a relaxation pathway are available, it will be preferable to excite one 1000 cm^{-1} vibration rather than ten 100 cm^{-1} phonons. The simplest relaxation pathway would involve the deposition of the initial vibrational energy into a single lower frequency vibration and one phonon. However, as shown by the INM calculations, neither CCl_4 nor CHCl_3 have phonon bandwidths that extend beyond 180 cm^{-1} . Therefore, in CHCl_3 , it is necessary for the initial vibration to relax into at least two vibrations and a phonon and in CCl_4 to relax into at least three vibrations and a phonon. This difference most likely is responsible for the generally longer relaxation times observed in CCl_4 . It is possible that it is necessary to excite more than one phonon to conserve energy. For simplicity, the following discussion assumes that only one phonon is involved, although this will not influence the conclusions that are reached.

The rate of vibrational relaxation, K , of the initially excited mode is generally described by Fermi's golden rule^{2,15,33}

$$K = \frac{2\pi}{\hbar} \sum_{r,r'} \rho_{r,r'} |\langle \sigma', r' | V | \sigma, r \rangle|^2. \quad (1)$$

In Eq. (1), σ and σ' denote the initial and final state of the initially excited vibration (the T_{1u} mode in this case), while r and r' refer to the receiving (or reservoir) modes (Fig. 7 and phonons). The ket $|\sigma, r\rangle$ is the initial state, described by thermal occupation numbers of the various modes of the system, in addition to unit occupation of the state initially excited by the ir pump. The bra $\langle \sigma', r' |$ is the final state with the initially populated state having occupation number 0 after relaxation and other states having increased occupation numbers. ρ is the density of states of the reservoir modes for the relaxation step, and is often written as a delta function to denote the energy conservation requirement. The summation in Eq. (1) denotes the fact that the true relaxation rate is a sum over contributions from all possible pathways; however, in the following discussion we will describe relaxation through a single anharmonic path involving one phonon.

In Eq. (1), V is the potential that describes the system–reservoir interaction. The potential energy surface for the system and reservoir is expanded about the potential minima $\{\psi_0\}$ of the various INM coordinates ψ_i

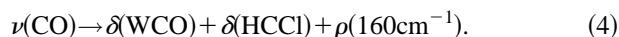
$$V = \sum_{\psi_i} V^{(2)} \cdot \psi^2 + \sum_{\psi_i} V^{(3)} \cdot \psi_1 \psi_2 \psi_3 + \dots, \quad (2)$$

where

$$V^{(i)} = \frac{\partial^i V}{\partial \psi_1 \dots \partial \psi_i} \Big|_{\{\psi_0\}} \dots \quad (3)$$

Here, $V^{(i)}$ is the i th matrix element that describes the interactions which couple i modes. The anharmonic terms, $i \geq 3$, govern relaxation processes involving the coupling of multiple vibrational modes. The magnitudes of the matrix element expansion coefficients decrease with order, leading to decreased relaxation rates with higher order processes.

As discussed above, given the vibrational energies of the solutes and the solvents, the relaxation of the initially excited mode results in the excitation of at least two other vibrations and a phonon. For such a process, the anharmonic coupling matrix element is at least fourth order, or quartic. For the following discussion, we use one of the quartic relaxation steps that contributes to the relaxation of the T_{1u} CO stretch in CHCl_3 . The CO stretch relaxes by transferring energy to the W–C–O bending motion of the $\text{W}(\text{CO})_6$, the H–C–Cl bending motion of the CHCl_3 , and a $\sim 160 \text{ cm}^{-1}$ solvent phonon. This quartic step can be written as



The quartic anharmonic matrix element $\langle V^{(4)} \rangle$ contains the magnitude of the quartic anharmonic coupling term, $|V^{(4)}|$, and combinations of raising and lowering operators that describe the anharmonic relaxation step. If the operator a annihilates the initially excited vibration and the operator b describes the change in the reservoir modes A , B , and the phonon, then the interaction is described by

$$a(b_A + b_A^+)(b_B + b_B^+)(b_{\text{ph}} + b_{\text{ph}}^+). \quad (5)$$

This interaction leads to seven possible quartic relaxation pathways,² some of which are unphysical. The relaxation pathway given by Eq. (4), a simple cascade process in which the energy relaxes only to lower energy modes, is described by one term arising from Eq. (5), $ab_A^+ b_B^+ b_{\text{ph}}^+$. Once substituted into Eq. (1), a raising operator brings out a factor of $\sqrt{n+1}$ and a lowering operator brings out a factor of \sqrt{n} , where n is the occupation number of the particular mode involved in the fourth order process. This allows Eq. (1) to be written as

$$K = \frac{2\pi}{\hbar} \rho_{\text{ph}} |\langle V^{(4)} \rangle|^2 (n_A + 1)(n_B + 1)(n_{\text{ph}} + 1), \quad (6)$$

where n is the thermally averaged occupation number,

$$n_i = (\exp(\hbar \omega_i / kT) - 1)^{-1}. \quad (7)$$

ω_i is the frequency of the vibrational or phonon mode. Our hypothesis is that $\rho_{\text{ph}} = \langle \rho(\omega_i) \rangle$, i.e., we apply the solid-state formalism to liquids. The question remains whether imaginary frequency modes ($\langle \rho(i\omega_i) \rangle$) contribute to ρ_{ph} .

Clearly, if the reservoir modes are high frequency ($\hbar \omega \gg kT$ and, therefore, $n \ll 1$), such as the discrete vibrational modes in Eq. 4, then Eq. 6 is

$$K = \frac{2\pi}{\hbar} \rho_{\text{ph}} |\langle V^{(4)} \rangle|^2 (n_{\text{ph}} + 1). \quad (8)$$

Although the discussion of the derivation of this relaxation rate expression has been qualitative, the same results can be shown rigorously.² In general, the expression for the relaxation rate along a given one-phonon, i th order anharmonic pathway is given by the product of the phonon density of states, the magnitude of the anharmonic coupling matrix element, and occupation number factors for the receiving modes. If a reservoir mode is created in the relaxation step, it contributes a factor of $(n + 1)$, whereas if it is annihilated, it contributes a factor of n . This is a simple, yet rigorous, method for describing even complex relaxation pathways.

Considering only the occupation number in Eq. (8), K should become larger and the observed decay times should become shorter as the temperature is increased. If more than one thermally occupied phonon were involved in the relaxation pathway or if a vibrational occupation number changes significantly, the temperature dependence would be even steeper. If the phonon occupation number is the only factor responsible for the temperature dependence, then for $\hbar\omega \ll kT$, K would increase linearly with temperature. For $\hbar\omega \gg kT$, K goes as $\exp(-\hbar\omega/kT)$ if a phonon is annihilated as part of the relaxation process, and K goes as $1 + \exp(-\hbar\omega/kT)$ if a phonon is created. In either limit and for intermediate situations, the temperature dependence of the occupation number(s) will always yield a decrease in the vibrational lifetime with increasing temperature. Only near $T \approx 0$ K (only phonon emission processes are possible) where $1 > n_{\text{ph}}$, will the temperature dependence vanish, and the vibrational lifetime will become temperature independent. Above $T \approx 0$ K, an inverted temperature dependence cannot be explained by considering occupation numbers, regardless of the pathways or number of modes involved.

The experimental data for $\text{W}(\text{CO})_6$ in CHCl_3 displayed in Fig. 3, with its inverted temperature dependence, show that the temperature dependence is influenced by temperature dependent factors in addition to the occupation numbers. A competition among these factors will yield the observed temperature dependence. The factors that cause the $\text{W}(\text{CO})_6/\text{CHCl}_3$ vibrational lifetimes to become longer as the temperature is increased are almost certainly operative in the other samples, such as $\text{W}(\text{CO})_6$ in CCl_4 , even though they do display vibrational lifetimes that decrease with increasing temperature.

The competition among factors can also be seen in the data in CCl_4 shown in Fig. 2, although it is not as obvious as in the $\text{W}(\text{CO})_6/\text{CHCl}_3$ data. The $\text{W}(\text{CO})_6/\text{CCl}_4$ data show an increase in the relaxation rate of 19% from the melting point to the boiling point. The minimum increase in vibrational relaxation rate with temperature due to the increase in thermal population can be shown to occur for a process in which the initially excited mode relaxes by creation of a high frequency vibration(s) ($\hbar\omega \gg kT$) and a single phonon. Any additional low frequency quanta will only cause a steeper increase in the rate with increasing temperature. For such a one phonon process, the change in thermal occupation number at the phonon cutoff of $\omega_D = 130 \text{ cm}^{-1}$ will cause an increase in

relaxation rate of 27% over the temperature range. A lower frequency phonon would produce a greater change, with a very low frequency phonon resulting in a 40% increase in rate. Since the experimental errors are very small, the 19% increase for $\text{W}(\text{CO})_6/\text{CCl}_4$ and the 16% increase for $\text{Cr}(\text{CO})_6/\text{CCl}_4$ demonstrate that additional factors must be offsetting the rate increases caused by the increasing occupation numbers to yield the observed temperature dependences.

In examining Eqs. (6) or (8), there are two other factors besides the occupation numbers that can contribute to the temperature dependence of the decay constant. They are the density of states, ρ , and the magnitude of the anharmonic coupling matrix element, $V^{(i)}$. First, consider the density of states. The densities of states of the internal vibrational modes of $\text{W}(\text{CO})_6$ do not change with temperature. However, the densities of states of the solvent modes will change with temperature; $\langle \rho(\omega) \rangle$ is temperature dependent at constant liquid density and, for the constant pressure case at hand, has additional temperature dependence through the temperature dependence of the liquid density. As the temperature increases, the liquid density decreases. The material densities for CCl_4 and CHCl_3 at room temperature are 1.592 and 1.480 g/cm^3 . While the densities are different, the temperature dependences are both linear and virtually identical, with a slope of $-0.002 \text{ g/cm}^3 \text{ K}$.³⁴ Therefore, any differences in the temperature-dependent density of states are unlikely to arise simply from a difference in the change in the number densities of particles in the two liquids. This applies to the solvent vibrations as well as the phonons. With this point in mind, let us now consider if differences in the temperature dependences of the $\langle \rho(\omega) \rangle$ in the two solvents can be responsible for the inverted temperature dependence observed in CHCl_3 .

As discussed above, calculations of the INMs display both real and imaginary frequencies.³⁻⁵ The real frequencies are true oscillations. The imaginary frequencies are related to potential barriers involved in structural evolution of the liquid. While it is still an open question, it might be expected that the real frequency part of the spectrum will be predominantly involved with the uptake of energy in vibrational relaxation. This is because the system spends most of its time near a potential minimum with infrequent excursions into the region of the potential associated with structural change. Thus, the real frequency modes are available for excitation during vibrational relaxation the majority of the time. In addition, the density of states of the imaginary part of the spectrum are peaked at significantly lower frequency than the real part. So if a moderately high frequency mode ($\sim 100 \text{ cm}^{-1}$) is required for energy conservation, the density of states will be much greater for the real part of the spectrum. For example, consider the relaxation pathway given in Eq. (4) for CHCl_3 . At the 160 cm^{-1} required phonon frequency, there is finite (but small) density of states in the real part of the spectrum but essentially zero density of states in the imaginary part of the spectrum.

Regardless of whether the imaginary modes can participate in vibrational relaxation, the conclusion will be the same. As discussed in Sec. III B, while there are some differences, the temperature-dependent behavior of the density

of INMs for the two solvents are very similar. If the same frequency phonon is involved in the relaxation in the two solvents, it is clear that the very small differences in the temperature dependences would not account for the different behaviors displayed in Figs. 2 and 3. However, it is unlikely that the same phonon frequency (or frequencies) will be involved. While the same internal modes of the $W(CO)_6$ are available in the two solvents, as can be seen in Fig. 7, the solvents have different high frequency modes available for participation in the relaxation pathways. Since different high frequency modes will be involved, the relaxation pathways will be substantially different and will involve phonons of different frequencies.

Can the temperature dependent changes in the density of states of $CHCl_3$ yield an inverted temperature dependence? The imaginary part of the spectrum has a density of states that increases with increasing temperature. Therefore, using a single phonon from the imaginary part of the density of states will only make the rate constant increase faster with increasing temperature than the phonon occupation number alone. The smallest change in the rate constant from a temperature dependent occupation number will occur for a single high frequency phonon. For the single path given in Eq. (4), the phonon frequency is 160 cm^{-1} . This is near the cutoff (see Fig. 5). It is approximately the highest frequency phonon that still has nonzero density of states. For this pathway, the change in the occupation number will cause the rate constant to increase by a factor of 1.33 going from the melting point (210 K) to the boiling point (334 K). Since a decrease in the rate constant of 9% is actually observed, the density of states would have to decrease by $\sim 40\%$. The calculations of the density of states do not cover the entire temperature range. However, the change over the lower half of the temperature range covered (260 to 300 K) is significantly less than the change over the upper half (300 to 340 K). The fact that the change is smaller at low temperature can perhaps be seen more clearly by looking at the imaginary part of the spectrum. The decrease in the real part results in an increase in the imaginary part as stable modes are replaced with unstable modes as the temperature is increased. Looking at the imaginary portions of Figs. 4 and 5, it is clear that there is a greater increase in the area at the higher temperatures. At the 160 cm^{-1} point in the real part of Fig. 5, there is very little change going from 260 to 340 K. Given the signal-to-noise ratio in the calculation, it is not clear that there is any change. It is expected that there will be no significant contribution to the total change from the range 210 to 260 K. Even around 50 cm^{-1} , where the decrease in the density of states is the largest, the decrease is never greater than 15%. With a 50 cm^{-1} phonon, it would require an $\sim 60\%$ decrease in phonon density of states to account for the observed data. If more than one phonon is involved, or if a phonon plus one of the very low frequency modes of $W(CO)_6$ (which are probably amalgamated with the INM) are in the relaxation pathway, the phonon occupation number contribution to the temperature dependence becomes steeper, and changes in the density of states are less able to compensate to yield the inverted temperature dependence. Therefore, changes in the density of states do not appear to be able to

account for the differences in the temperature dependences observed in CCl_4 and $CHCl_3$ or for the inverted temperature dependence observed in $CHCl_3$.

The discussion above implicitly assumes delta function transition frequencies for the discrete vibrational modes and the liquids phonons. This limit is equivalent to assuming that spectral lines are delta functions. For the phonons, the linewidths are not significant since there is already a continuum of states. Vibrational lines of molecules in liquids show significant line widths. Depending on the system and the temperature, the vibrational lines can have significant homogeneous linewidths, although the observed linewidth may have a significant contribution from or be dominated by inhomogeneous broadening. A finite homogeneous linewidth is caused by the vibrational lifetime and additional processes such as pure dephasing and orientational relaxation. Although vibrational transitions in liquids may be inhomogeneously broadened,^{10,35,36} the homogeneous linewidth in liquids can be a significant fraction of the total spectral width. The issue of homogeneous broadening in low frequency solvent modes is only beginning to be explored.³⁷⁻³⁹ The finite width of vibrational lines will lead to relaxation of the energy matching requirement of the relaxation pathways, as the combined spectral overlap will determine the efficiency of the relaxation processes. However, at room temperature, the homogeneous linewidth can range from as little as 1 to $\sim 10\text{ cm}^{-1}$. Since a homogeneous linewidth of 10 cm^{-1} is small compared to the phonon bandwidths, for a process that involves one or more phonons, the homogeneous width will not be of great importance. However, if there is a near match of the sum of discrete vibrational energies with the energy of the initially excited state, a significant homogeneous width could open up a pathway that would otherwise be forbidden. In general, the homogeneous linewidth will increase with increasing temperature. Therefore, a pathway that is forbidden at low temperature could turn on as the temperature is increased. This would increase the rate of vibrational relaxation and cannot explain the inverted temperature dependence. It is possible for motional narrowing to occur with increased temperature. The narrowing of a vibrational line could turn off a pathway with increasing temperature. This could produce an inverted temperature dependence, but it would require very special circumstances. There would have to be a match in energies at low temperature not involving the INM continuum, and motional narrowing would have to occur to eliminate this match. While this is possible, it does not apply to the experimental systems discussed here. There is no indication of motion narrowing in the temperature dependent line shapes. Also, we see the inverted temperature dependence or evidence of the offsetting influence that compensates for the temperature dependence of the occupation numbers in many systems, i.e., $W(CO)_6$ and $Cr(CO)_6$ in CCl_4 and $CHCl_3$ and in other solvents. These have different internal modes and different solvent modes. For everyone of these to have a pathway that conserves energy without employing the low frequency continuum of INM and that turns off because of motional narrowing, is essentially impossible.

In the above, we have argued that it is not possible to account for the inverted temperature dependence or even the

noninverted temperature dependences considering only the temperature dependent occupation numbers. These always give an increase in rate with temperature, so cannot account for the inverted temperature dependence, and given the high frequency cutoffs of the INMs, the noninverted temperature dependences are too mild to be accounted for by occupation numbers alone. Then, considering the temperature dependences of the density of states of the INMs, it is still not possible to account for the inverted temperature dependence. Returning to Eq. (8), the remaining factor is the influence of temperature on the magnitude of the anharmonic coupling matrix element, $V^{(i)}$.

The results suggest that a significant temperature dependence exists for the magnitude $V^{(i)}$. The temperature dependence of this term must be opposite to that of the phonon occupation numbers and must be sufficiently large to offset the change in occupation numbers to yield the inverted temperature dependence. Although $V^{(i)}$ is not explicitly temperature dependent, it can vary with density. Calculations for molecular crystals have shown that this density dependence can be significant.⁴⁰ As the density decreases with increasing temperature, intermolecular separations are increased on average. There is a multiplicative factor of the density in $V^{(i)}$, which we have seen has almost identical temperature dependence in the two solvents. More importantly the region of the intermolecular potential sampled changes, and therefore the anharmonic coupling matrix elements can change with a strong temperature dependence. If this causes the matrix elements to become smaller with increasing temperature, then this decrease will work to offset the increase in occupation numbers. If this effect is sufficiently large, the observed inverted temperature dependence of $W(\text{CO})_6/\text{CHCl}_3$ would be observed. This is the most likely explanation for the inverted temperature dependence.

There are two possible reasons why the observed behaviors in CCl_4 and CHCl_3 are so different. The vibrational relaxation pathways in the two solvents will be different. In CHCl_3 , the quartic process given in Eq. (4) could provide an efficient, relatively low order, pathway. This uses the high frequency CH mode of CHCl_3 not available in CCl_4 . Since different modes are involved in the solvents, there could be a significant difference in the influence of changes in density on the matrix elements in the two solvents. If the pathways in both solvents only involve a single phonon, despite the large differences in available internal frequencies, the change in occupation numbers will be similar. This would imply that change in the matrix element in CHCl_3 is much larger than in CCl_4 , the difference being large enough to yield the inverted temperature dependence in CHCl_3 but only resulting in a partial compensation for the occupation number change in CCl_4 .

The other possibility is that there is approximately the same decrease in the coupling matrix elements in the two solvents, but the occupation number contributions are very different. As discussed above, a single phonon pathway yields the most mild occupation number contribution to the temperature dependence. If, in CHCl_3 , the relaxation path involves a single phonon and the decrease in the coupling matrix elements with temperature is sufficiently large, the

inverted temperature dependence results. However, if, in CCl_4 , the relaxation pathway uses two phonons, the occupation number contribution to the temperature dependence will be much steeper. Then the decrease in the coupling matrix elements may only partially overcome the temperature dependence, yielding a mild dependence but not an inverted dependence. At present, it is not possible to distinguish these two possibilities.

V. CONCLUDING REMARKS

Examination of the temperature dependences of the T_{1u} CO stretching mode of $W(\text{CO})_6$ in CCl_4 and CHCl_3 from the melting points to the boiling points of the solvents and consideration of the temperature dependences and the calculated INM spectra for the liquids yield detailed insights into the nature of vibrational dynamics in liquids. The observation that the vibrational lifetime of $W(\text{CO})_6$ in CHCl_3 actually becomes longer as the temperature increases (inverted temperature dependence) demonstrates that lifetimes are not simply controlled by an activation energy. Examination of the temperature dependence in CCl_4 revealed a temperature dependence that is too mild to be accounted for by changes in occupation numbers alone. This was made possible by the calculation of the INM spectrum, which provides the maximum phonon frequency that can be involved in the relaxation.

Three factors were discussed that will influence the vibrational lifetime of the metal carbonyls studied and, presumably, other systems as well. They are (1) the temperature-dependence occupation number of the phonon(s) or other very low frequency modes excited in the relaxation of the initially pumped vibration; (2) the temperature dependence of the liquid's density of INM states; and (3) the temperature dependence of the magnitude of the anharmonic coupling matrix elements responsible for vibrational relaxation.

Calculation of the INM spectrum for CHCl_3 demonstrates that temperature-dependent changes in the phonon density of states are not sufficiently large to explain the inverted temperature dependence. Rather, it is possible that changes in liquid density with temperature results in a reduction in the strength of coupling between the initially excited mode and the receiving modes. In CHCl_3 , the reduction in the anharmonic coupling matrix elements are large enough to overcome the increase in occupation numbers with increasing temperature, yielding the observed inverted temperature dependence. Clearly, the next step for applying instantaneous normal mode analysis to the problem of vibrational lifetimes is evaluation of the anharmonic coupling; we intend to do this with simulations explicitly incorporating the solute. INM studies of solute-solvent systems have already been performed,⁴¹ but coupling constants, such as those under discussion in this paper, have not been calculated.

Another consideration which we have not discussed is that coupling to some types of solvent modes may be more important than to others. In our discussion of the spectra of INM, we analyzed the effect of different energies on the temperature dependence, tacitly assuming that the coupling mechanism would not select out a particular type of mode,

e.g., translation or rotation. If the $LJ\langle\rho(\omega)\rangle$ in Fig. 6 represents the true translational $\langle\rho(\omega)\rangle$, then, e.g., relaxation dominated by translational modes would employ this relatively low $\omega\langle\rho(\omega)\rangle$ for ρ_{ph} . This would further limit the range of frequencies of the continuum available for energy conservation. The possibility of selective coupling does not change any of the conclusions that have been presented.

The results presented here demonstrate that understanding the temperature dependence of vibrational lifetimes requires consideration of the interplay of the temperature dependences of the occupation number, the density of states, and the coupling matrix elements. Observation of a normal (noninverted) temperature dependence does not indicate that all three factors are not involved. Fitting a normal temperature dependence as a simple activated process can yield a highly flawed indication of the frequency of the low frequency mode that is involved.

ACKNOWLEDGMENTS

A.T. and M.D.F. acknowledge support for this work by the National Science Foundation (DMR93-22504), the Office of Naval Research (N00014-92-J-1227), and the Air Force Office of Scientific Research (F49620-94-1-0141). T.K. acknowledges support by the National Science Foundation (CHE94-15216), and would like to thank Prof. R. M. Stratt for many useful discussions pertaining to this work.

- ¹A. Tokmakoff, B. Sauter, and M. D. Fayer, *J. Chem. Phys.* **100**, 9035 (1994).
- ²V. M. Kenkre, A. Tokmakoff, and M. D. Fayer, *J. Chem. Phys.* **101**, 10618 (1994).
- ³G. Seeley and T. Keyes, *J. Chem. Phys.* **91**, 5581 (1989).
- ⁴B. C. Xu and R. M. Stratt, *J. Chem. Phys.* **92**, 1923 (1990).
- ⁵T. M. Wu and R. M. Loring, *J. Chem. Phys.* **97**, 8568 (1992).
- ⁶P. Moore and T. Keyes, *J. Chem. Phys.* **100**, 6709 (1993).
- ⁷M. Cho, G. R. Fleming, S. Saito, I. Ohmine, and R. M. Stratt, *J. Chem. Phys.* **100**, 6672 (1994).
- ⁸T. Keyes, *J. Chem. Phys.* **101**, 5081 (1994).
- ⁹A. Tokmakoff, R. S. Urdahl, D. Zimdars, R. S. Francis, A. S. Kwok, and M. D. Fayer, *J. Chem. Phys.* **102**, 3919 (1995).
- ¹⁰A. Tokmakoff and M. D. Fayer, *J. Chem. Phys.* (to be published).
- ¹¹D. J. Diestler, *Adv. Chem. Phys.* **42**, 305 (1980).

- ¹²A. Nitzan and J. Jortner, *Mol. Phys.* **25**, 713 (1973).
- ¹³A. Nitzan and R. J. Silbey, *J. Chem. Phys.* **60**, 4070 (1974).
- ¹⁴D. J. Diestler, *J. Chem. Phys.* **60**, 2692 (1974).
- ¹⁵D. W. Oxtoby, *Adv. Chem. Phys.* **47**, 487 (1981).
- ¹⁶J. Chesnoy and G. M. Gale, *Adv. Chem. Phys.* **70**, 297 (1988).
- ¹⁷S. A. Adelman, R. Muralidhar, and R. H. Stote, *J. Chem. Phys.* **95**, 2738 (1991).
- ¹⁸A. Tokmakoff, C. D. Marshall, and M. D. Fayer, *J. O. S. A. B* **10**, 1785 (1993).
- ¹⁹M. Iannone, B. R. Cowen, R. Diller, S. Maiti, and R. M. Hochstrasser, *Appl. Opt.* **30**, 5247 (1991).
- ²⁰M. Tuckerman, G. J. Martyna, and B. Berne, *J. Chem. Phys.* **97**, 1990 (1992).
- ²¹G. J. Martyna, M. Tuckerman, and M. L. Klein, *J. Chem. Phys.* **101**, 4177 (1994).
- ²²G. J. Martyna, M. Tuckerman, and M. L. Klein, *J. Chem. Phys.* **97**, 2635 (1992).
- ²³W. Dietz and K. Heinzinger, *Ber. Bunsenges. Phys. Chem.* **88**, 546 (1984).
- ²⁴Gerhard Herzberg, *Molecular Spectra and Molecular Structure* (Prentice-Hall, New York, 1939).
- ²⁵H. L. Jones, *Spectrochim. Acta* **19**, 329 (1963).
- ²⁶J. M. Smith and L. H. Jones, *J. Mol. Spectrosc.* **20**, 248 (1966).
- ²⁷L. H. Jones, R. S. McDowell, and M. Goldblatt, *Inorg. Chem.* **8**, 2349 (1969).
- ²⁸D. M. Adams and I. D. Taylor, *J. Chem. Soc., Faraday Trans. 2* **78**, 1051 (1982).
- ²⁹R. L. Amster, R. B. Hannan, and M. C. Tobin, *Spectrochim. Acta* **19**, 1489 (1963).
- ³⁰J. R. Madigan, *J. Chem. Phys.* **19**, 119 (1951).
- ³¹J. P. Zietlow, F. F. Cleveland, and A. G. Meister, *J. Chem. Phys.* **18**, 1076 (1950).
- ³²S. R. J. Brueck and R. M. Osgood, *Chem. Phys. Lett.* **39**, 568 (1976).
- ³³D. W. Oxtoby, *Annu. Rev. Phys. Chem.* **32**, 77 (1981).
- ³⁴S. O. Morgan and H. H. Lowry, *J. Phys. Chem.* **34**, 2416 (1930).
- ³⁵D. Zimdars, A. Tokmakoff, S. Chen, S. R. Greenfield, M. D. Fayer, T. I. Smith, and H. A. Schwettman, *Phys. Rev. Lett.* **70**, 2718 (1993).
- ³⁶A. Tokmakoff, D. Zimdars, B. Sauter, R. S. Francis, A. S. Kwok, and M. D. Fayer, *J. Chem. Phys.* **101**, 1741 (1994).
- ³⁷Y. Tanimura and S. Mukamel, *J. Chem. Phys.* **99**, 9496 (1993).
- ³⁸K. Tominaga, Y. Naitoh, T. J. Kang, and K. Yoshihara, in *Ultrafast Phenomena IX*, edited by G. Mourou, A. H. Zewail, P. F. Barbara, and W. H. Knox (Springer, Berlin, 1994).
- ³⁹S. Palese, J. T. Buontempo, L. Schilling, W. T. Lotshaw, Y. Tanimura, S. Mukamel, and R. J. D. Miller, *J. Phys. Chem.* **98**, 12466 (1994).
- ⁴⁰Andrei Tokmakoff, M. D. Fayer, and Dana D. Dlott, *J. Phys. Chem.* **97**, 1901 (1993).
- ⁴¹R. M. Stratt and M. Cho, *J. Chem. Phys.* **100**, 6700 (1994); S. J. Schvaneveldt and R. F. Loring, *ibid.* **102**, 2326 (1995); B. M. Ladanyi and R. M. Stratt, *J. Phys. Chem.* **99**, 2502 (1995).